

Phase diagram for asymmetric nuclear matter in the multifragmentation modelG. Chaudhuri¹ and S. Das Gupta²¹*Variable Energy Cyclotron Centre, 1/AF Bidhan Nagar, Kolkata 700064, India*²*Physics Department, McGill University, Montréal, Quebec H3A 2T8, Canada*

(Received 10 August 2009; published 15 October 2009)

We assume that, in equilibrium, nuclear matter at reduced density and moderate finite temperature breaks up into many fragments. Strong support for this assumption is provided by data accumulated from intermediate-energy heavy ion collisions. The breakup of hot and expanded nuclear matter according to the rules of equilibrium statistical mechanics is the multifragmentation model, which gives a first-order phase transition. This is studied in detail here. Phase-equilibrium lines for different degrees of asymmetry are computed.

DOI: [10.1103/PhysRevC.80.044609](https://doi.org/10.1103/PhysRevC.80.044609)

PACS number(s): 25.70.Mn, 25.70.Pq

I. INTRODUCTION

Nuclear matter is a hypothetical very large system of nucleons in which the Coulomb effects of protons are switched off. Such a system is expected to have features of liquid-gas phase transition. We consider here the equation of state of symmetric and asymmetric nuclear matter at temperatures between 4 and 10 MeV and at less than half of normal nuclear density. We assume that at equilibrium at finite temperature (three to tens of MeV) and low average density, nuclear matter breaks up into fragments, each with normal nuclear density. Strong support for this assumption comes from data on heavy ion collisions, but it is also supported by theoretical modeling. For example, it can be easily shown (see Sec. IV in Ref. [1]), using a Skyrme type interaction, that the free energy of uniformly stretched nuclear matter is very significantly lowered if the matter is allowed to split into many fragments, each with normal nuclear density. This is the multifragmentation model. We use this model to study thermodynamic properties of nuclear matter, particularly phase-equilibrium lines (the lines of coexistence of liquid and gas phases) in the p - T plane for both symmetric and asymmetric matter.

This is an extension of the model described in our earlier work [2], which considered only one kind of particle. These particles, however, formed clusters whose properties were patterned after actual finite nuclei. While we hope that the present article is self-contained, we will refer to this earlier work for elucidation of some points. There is a large number of publications on equation of state and phase transitions in nuclear matter. Reference [3] comes closest to the spirit of this paper. While it has quite a few common features with this work, there are also some differences and we highlight some other aspects. Phase transition in nuclear matter using mean-field theory has been studied for many years, and we cannot attempt to give an adequate bibliography here. We mention two papers that critically examined asymmetric nuclear matter and received a great deal of attention in very recent times [4,5]. Both of these used mean-field theories and overcame the difficulty of instability through Maxwell construction. The multifragmentation approach is very different. It is more directly related to actual observables, but in its present form it can only be trusted in a low-density regime. However, there is no need for Maxwell construction.

II. THE FORMULAS

We briefly review the grand canonical model for multifragmentation [6]. Let the number of neutrons and protons in the dissociating system be N_0 and Z_0 , respectively. At finite temperature and in subnormal densities, these will break up into all possible composites each with some neutrons N and protons Z (mass number $A = N + Z$). We always use the subscripted N_0, Z_0 to refer to the very large system whose thermodynamic properties are being investigated, whereas N, Z refer to composites that can be small or large. The properties of the composites are determined by the basic two-body interactions. These properties are utilized in the model, but interactions between composites are neglected (except through excluded volume effect; see discussion later) by appealing to the short-range nature of nuclear forces. This limits the validity of the model to low densities. Here we will restrict our investigation to densities ρ/ρ_0 to 0.5 or less, where ρ_0 is the normal nuclear density. This is the customary practice [7].

If the neutron chemical potential is μ_n and the proton chemical potential is μ_p , then statistical equilibrium implies that the chemical potential of a composite with N neutrons and Z protons is $\mu_n N + \mu_p Z$. The following are the relevant equations for us. The average number of composites with N neutrons and Z is ($\beta = 1/T$)

$$\langle n_{N,Z} \rangle = e^{\beta \mu_n N + \beta \mu_p Z} \omega_{N,Z}. \quad (1)$$

Here $\omega_{N,Z}$ is a one-body partition function for the composite (N, Z). It is a product of two factors; one arising from the translational motion of the composite and another from the intrinsic partition function of the composite:

$$\omega_{N,Z} = \frac{V_f}{h^3} (2\pi m T)^{3/2} A^{3/2} \times z_{N,Z}(\text{int}). \quad (2)$$

Here V_f is the volume available for translational motion; V_f will be less than V , the volume to which the system has expanded at breakup (excluded volume correction). We use $V_f = V - V_0$, where V_0 is the normal volume of nucleus with Z_0 protons and N_0 neutrons. The quantity $z_{N,Z}(\text{int})$ depends upon the intrinsic properties of the composites and contains all the nuclear physics.

We list now the properties of the composites used in this work. The proton and the neutron are fundamental building

blocks, thus $z_{1,0}(\text{int}) = z_{0,1}(\text{int}) = 2$, where 2 takes care of the spin degeneracy. For deuteron, triton, ${}^3\text{He}$, and ${}^4\text{He}$, we use $z_{i,j}(\text{int}) = (2s_{i,j} + 1) \exp(-\beta e_{i,j}(\text{gr}))$, where $e_{i,j}(\text{gr})$ is the ground state energy of the composite and $(2s_{i,j} + 1)$ is the experimental spin degeneracy of the ground state. Because we are modeling a system in which protons do not carry any charges, the ground state energy of ${}^3\text{He}$ is taken to be that of the triton, and the Coulomb energy is subtracted from the experimental energy of the α particle. These modifications make insignificant changes. Excited states for these very low mass nuclei are not included. For mass number $a = 5$ and greater, we use the liquid-drop formula. This reads

$$z_{i,j}(\text{int}) = \exp\left[-\frac{F_{i,j}}{T}\right]. \quad (3)$$

Here $F_{i,j}$ is the internal free energy of species (i, j) :

$$F_{i,j} = -W_0 a + \sigma(T) a^{2/3} + s \frac{(i-j)^2}{a} - \frac{T^2 a}{\epsilon_0}. \quad (4)$$

The expression includes the volume energy, the temperature-dependent surface energy, and the symmetry energy. The values of the parameters are taken from Ref. [8]. The term $\frac{T^2 a}{\epsilon_0}$ represents contribution from excited states, since the composites are at a nonzero temperature. For nuclei with $A = 5$, we include $Z = 2$ and 3; and for $A = 6$, we include $Z = 2, 3$, and 4. For higher masses, we compute the drip lines using the liquid-drop formula above and include all isotopes within these boundaries.

There are two equations that determine μ_n and μ_p :

$$N_0 = \sum N e^{\beta \mu_n N + \beta \mu_p Z} \omega_{N,Z}, \quad (5)$$

$$Z_0 = \sum Z e^{\beta \mu_n N + \beta \mu_p Z} \omega_{N,Z}. \quad (6)$$

We want to point out the following feature of the grand canonical model. In all $\omega_{N,Z}$ in the sum in the above two equations, there is one common value for V_f [see Eq. (2)]. We really solve for N_0/V_f and Z_0/V_f . The values of μ_n or μ_p will not change if we, say, double N_0 , Z_0 , and V_f simultaneously provided the number of terms in the sum is unaltered. We then might as well say that when we are solving the grand canonical equation, we are really solving for an infinite system (because we know that fluctuations will become unimportant), but this infinite system can break up into only the kinds of species that are included in Eqs. (5) and (6). Which composites are included in the sum is an important physical ingredient in the model, but intensive quantities such as β , μ depend not on N_0 , Z_0 but on N_0/V_f and Z_0/V_f .

The choice of which nuclei are included in the sum of the right-hand side of Eqs. (5) and (6) needs further elucidation. We can look upon the sum on N and Z as a sum over A and a sum over Z . In principle, A goes from 1 to ∞ ; and for a given A , Z can go from 0 to A . Here for a given A , we restrict Z by the drip lines. Comparisons with calculations that do not impose restrictions by drip lines (as in the Copenhagen statistical multifragmentation model) showed that restrictions by drip lines generate imperceptible differences [9]. De and Samaddar [3] reached a similar conclusion.

Let us now consider the restriction on A . In principle, this should be ∞ , but for practical calculations one needs to restrict this to a maximum value that we label as A_{max} . Earlier calculations with one kind of particles showed that with $A_{\text{max}} = 200$, features of the liquid-gas phase transition are not revealed (see Fig. 14 in Ref. [7]), but a high value of $A_{\text{max}} = 2000$ produces a nearly perfect model of phase transition (elaborated in much greater detail in Refs. [2,3]).

III. SIGNATURES OF PHASE TRANSITION IN THE MODEL

We now demonstrate that the multifragmentation model predicts the first-order phase transition. There are three signatures we will dwell on. Pressure in the model is given by $p = T \frac{\sum n_{N,Z}}{V_f} = T \frac{\sum n_A/A_0}{V_f/A_0} = T \rho_f \frac{\sum n_A}{A_0}$. We plot our results as functions of ρ rather than ρ_f the connection being $\rho_f = \frac{\rho \rho_0}{\rho_0 - \rho}$. We have $\rho = \rho_n + \rho_p$. We need an asymmetry parameter. We use both N_0/Z_0 and $\omega = \frac{N_0 - Z_0}{N_0 + Z_0}$.

We show in Fig. 1 the p - ρ curves for $N_0/Z_0 = 1.4$, where the values of A_{max} are 200, 400, 600, 800, and 1000. The temperature used is $T = 6.5$ MeV. For all five choices of A_{max} , the pressure against ρ initially rises quite sharply and then flattens out considerably. The initial stage of the fast rise of pressure with density is the gas phase. Here the results do

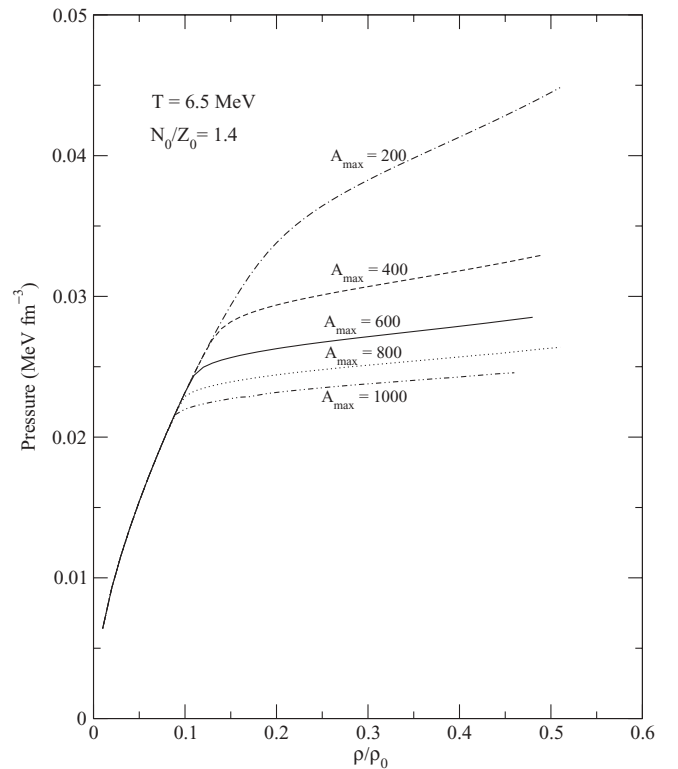


FIG. 1. Pressure-density curves for $N_0/Z_0 = 1.4$ and $T = 6.5$ MeV, where the values of A_{max} used are 200, 400, 600, 800, and 1000. Note that in the region of fast pressure rise with density, results are insensitive to A_{max} . In the high-density side, pressure appears to approach a constant value as a function of density as A_{max} increases.

not matter whether A_{\max} is 200, 400, or larger. The reason will become clearer later (it is explained in detail in Ref. [2]). The flattening that follows depends on A_{\max} , but above a large enough value of A_{\max} , it will not change. For one kind of particle, this is reached around 2000 [2]. However, the choice of $A_{\max} = 600$ is good enough for at least a semiquantitative estimate of various thermodynamic properties of nuclear matter, and we will present results for this value, although we did some calculations with other choices of A_{\max} also. The flattening happens slightly beyond $\rho/\rho_0 = 0.1$. We show results up to $\rho/\rho_0 = 0.5$, arguing that the excluded volume correction for interactions between composites becomes worse with increasing density.

The rise of pressure at small density followed by a flattening of p with increasing density is a signature of a first-order liquid-gas transition. We have shown results for $T = 6.5$ MeV. Beyond a certain temperature, the flatness will disappear, showing that there is no more phase transition in the domain $\rho/\rho_0 \leq 0.5$. Similarly, the flattening of p disappears beyond some value of N_0/Z_0 . The liquid-drop parameters we are using give us for large nuclei the drip line at N/Z (and of course Z/N) about 2. Hence for larger values of N_0/Z_0 , the system cannot stay together even at $T = 0$. Then we will have a system that has a bound core but always many free nucleons, which will dominate the thermodynamic properties of the system.

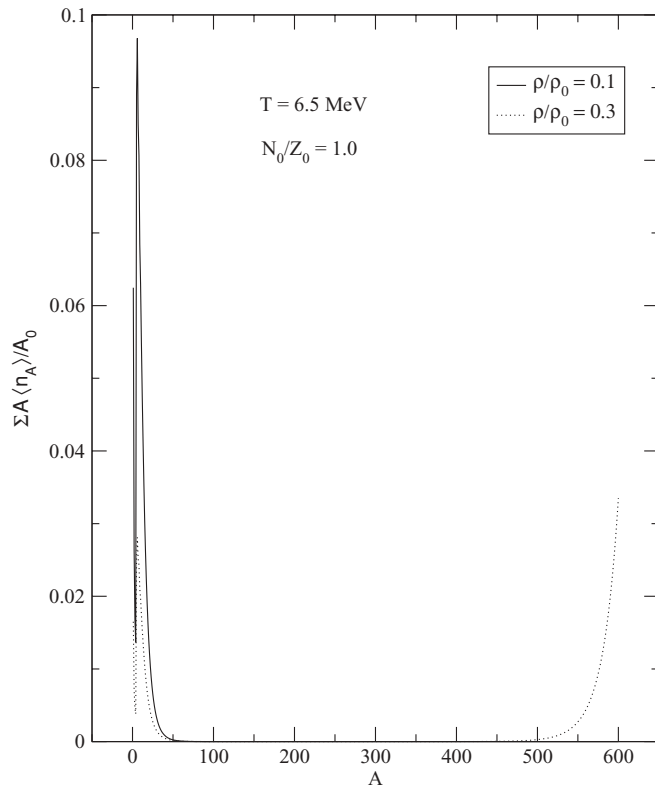


FIG. 2. $A\langle n_A \rangle/A_0$ as a function of the mass number A for $N_0/Z_0 = 1.0$ and $T = 6.5$ MeV. For the distribution of composites at $\rho/\rho_0 = 0.1$ (solid line), there are practically no heavy particles, none above $A = 70$; this is a pure gas phase. At $\rho/\rho_0 = 0.3$ (dotted line), there are both light and heavy ($A \geq 500$) particles; this is coexistence. Here and in the rest of the figures, we used $A_{\max} = 600$.

This is not a system we want to study. Hence in this work, we constrained ourselves to a system whose N_0/Z_0 spans 1.0–1.8. The upper limit is indeed a highly asymmetric system.

Below the density at which the phase transition sets in, the system is in a pure gas phase. At the phase transition point, some liquid will be formed, and the fraction of nucleons in the liquid phase will grow at the expense of the gas particles as the density increases. This can actually be followed. One also gets a functional definition of what constitutes the gas particles. Here our identification is very different from what was concluded in Ref. [3] but very similar to what was found in our earlier work with one kind of particle [2].

Lastly, in a one-component model, there is just one μ , which stays constant throughout the coexistence region. Now there are two chemical potentials μ_n and μ_p . How do they behave?

IV. WHAT CONSTITUTES THE GAS AND WHAT CONSTITUTES THE LIQUID?

The quantity $\langle n_A \rangle \equiv \sum_{N+Z=A} \langle n_{N,Z} \rangle$ is the average number of composites with mass number A . The quantity $A\langle n_A \rangle/A_0$ gives the fraction of particles tied up in composites with mass number A . This is plotted in Figs. 2 and 3 for $N_0/Z_0 = 1.0$ and $N_0/Z_0 = 1.8$, respectively. First concentrating on Fig. 2 ($T = 6.5$ MeV), we see that at density $\rho/\rho_0 = 0.1$ the nucleons are bound in composites ≤ 50 . These particles constitute the gas phase. At density $\rho/\rho_0 = 0.3$, some heavy composites with $A \approx A_{\max}$ begin to form, and the probability of such heavy

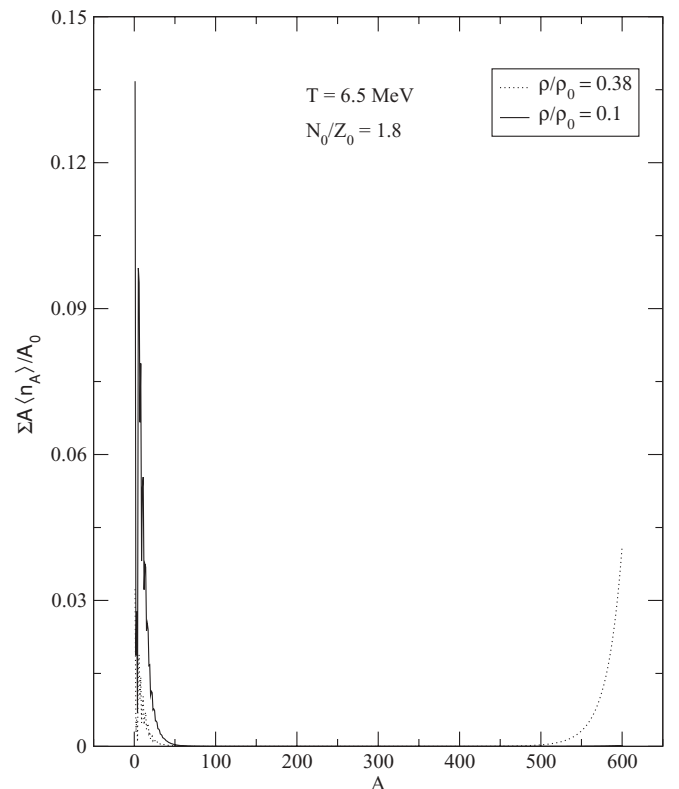


FIG. 3. Same as Fig. 2, but for $N_0/Z_0 = 1.8$; dotted line is for $\rho/\rho_0 = 0.38$.

particles (with A between A_{\max} and $A_{\max} - 100$) begins to increase (at the expense of the light particles) as the density increases. This is a clear evidence of coexistence. We thus consider light particles ($A \leq 70$) to be gas and heavier particles (with A between A_{\max} and $A_{\max} - 135$) to be liquids. Figure 3 displays similar physics but for $N_0/Z_0 = 1.8$: all gas particles at $\rho/\rho_0 = 0.1$ and a mixture of gas and liquid at $\rho/\rho_0 = 0.38$.

We note that even the gas phase in the fragmentation model is quite complicated. It is not just neutrons and protons but other light nuclei as well. In addition, during coexistence, the isotopic content of the gas phase changes continuously as the volume of the container, i.e., density ρ/ρ_0 changes. This is called isospin fractionation and is well-known in the literature. We will briefly come back to this aspect later.

V. CHEMICAL POTENTIALS

In numerical work involving only one kind of particle [2], it was demonstrated that in the limit of $A_{\max} \rightarrow \infty$, a constant value of μ will be achieved in the coexistence region. This value could be obtained by extrapolation. In the present case, there are two chemical potentials. For $N_0/Z_0 \neq 1$, $\mu_n \neq \mu_p$. For $N/Z = 1.4$ and temperature 6.5 MeV, we show in Fig. 4 the evolution of μ_n and μ_p as a function of density. One notices

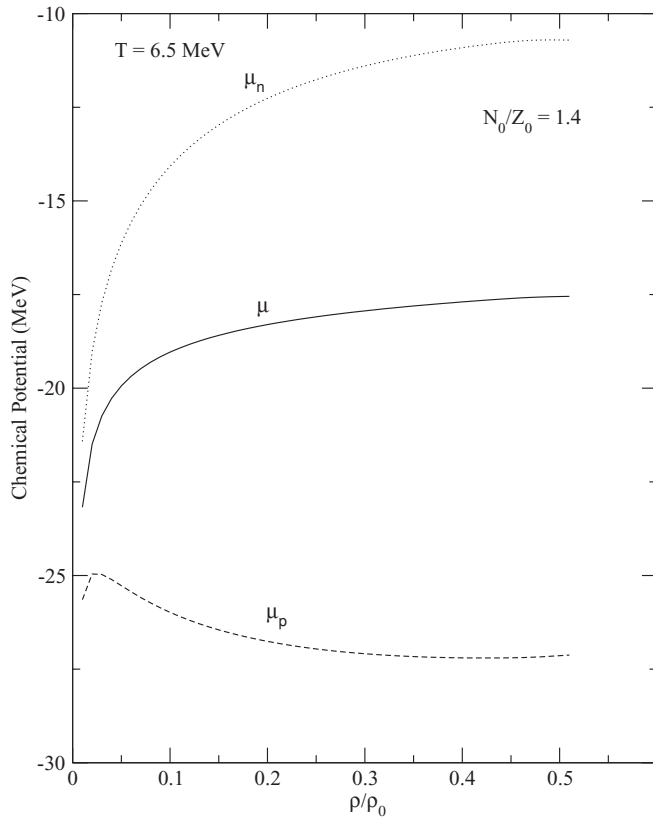


FIG. 4. Chemical potential as function of density for $N_0/Z_0 = 1.4$ and $T = 6.5$ MeV. The dotted line is the neutron chemical potential μ_n , the dashed line is the proton chemical potential μ_p , and the solid line is $\mu = \frac{N_0}{A_0}\mu_n + \frac{Z_0}{A_0}\mu_p$.

that both μ_n and μ_p change rapidly in the gas phase and then tend to a constant value. In the limit $A_{\max} \rightarrow \infty$, we expect they will become constants. We also plot in the same figure $\mu \equiv \frac{N_0}{N_0+Z_0}\mu_n + \frac{Z_0}{N_0+Z_0}\mu_p$. The μ so defined has a meaning at the three limits: -1 , 0 , and $+1$ for asymmetry parameter $\omega = \frac{N_0-Z_0}{N_0+Z_0}$; it is interesting to note that μ tends to a constant value faster than either μ_n or μ_p .

VI. COEXISTENCE LINES

Figure 5 shows that as the temperature increases, phase coexistence finally disappears (from the region $\rho/\rho_0 \leq 0.5$). We have shown this for $N_0/Z_0 = 1.0$, but this is also true for asymmetric systems provided the asymmetry is not too large, as explained earlier.

We show in Fig. 6 the p - ρ curves at $T = 6.5$ MeV for three systems with $N_0/Z_0 = 1, 1.4$, and 1.8 . We identify as A, B, and C the points on these curves at which coexistence sets in. The values of pressure at these points give us p values for coexistence at this temperature for these N_0/Z_0 values. This is not strictly correct. The values of p increase slightly as one moves toward higher density. This is because with $A_{\max} = 600$, we have not yet reached asymptotic limits. However, this is adequate for our purposes. Repeating this analysis for different temperatures, we obtain coexistence lines in the T - p plane for nuclear matter with different asymmetries

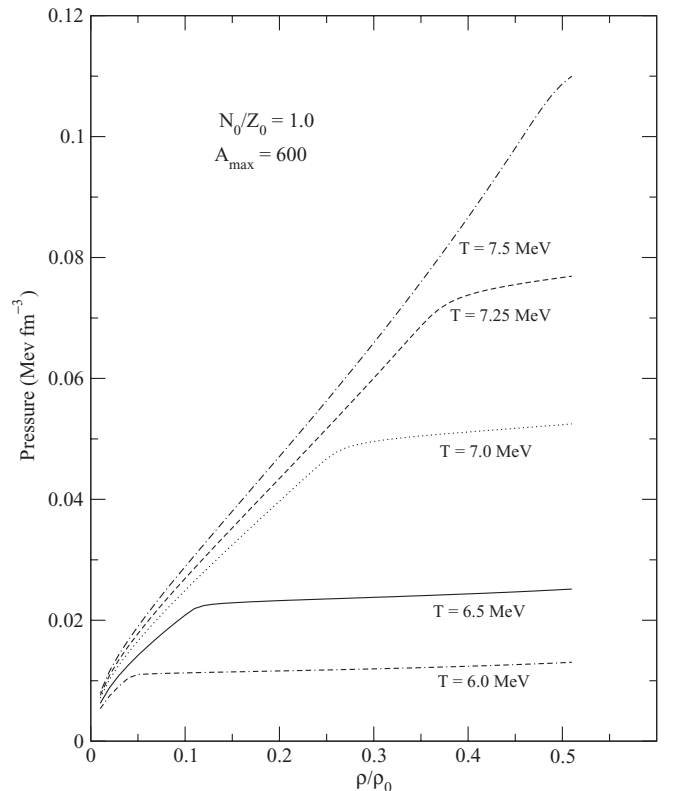


FIG. 5. Pressure-density isotherms at $T = 6, 6.5, 7.0, 7.25$, and 7.5 MeV for $N_0/Z_0 = 1.4$ and $A_{\max} = 600$. Note that the point of the beginning of coexistence moves up and to the right as the temperature increases.

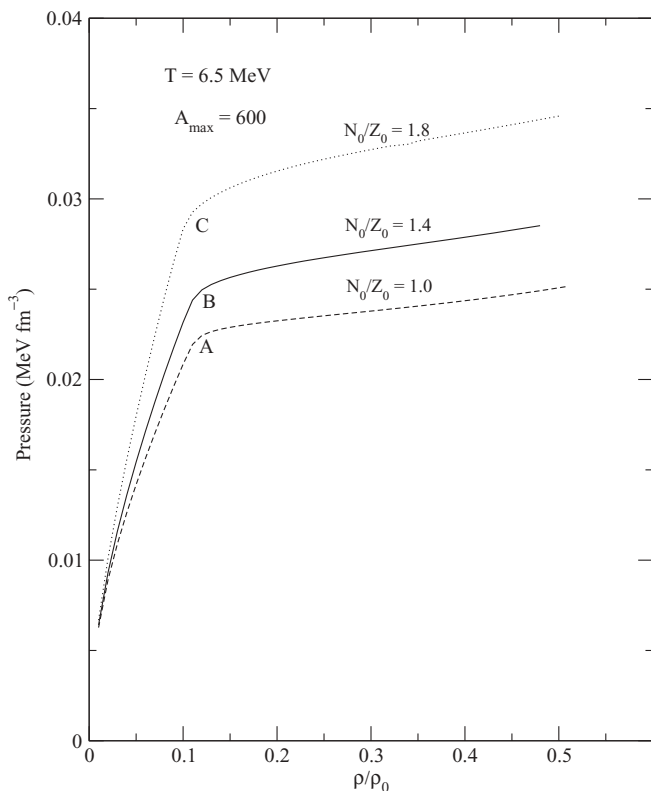


FIG. 6. Pressure-density curves at $T = 6.5$ MeV for three systems with (N_0/Z_0) values equal to 1, 1.4, and 1.8. Points A, B, and C on the isotherms will give the values of pressure when coexistence sets in at $T = 6.5$ MeV for these N_0/Z_0 values.

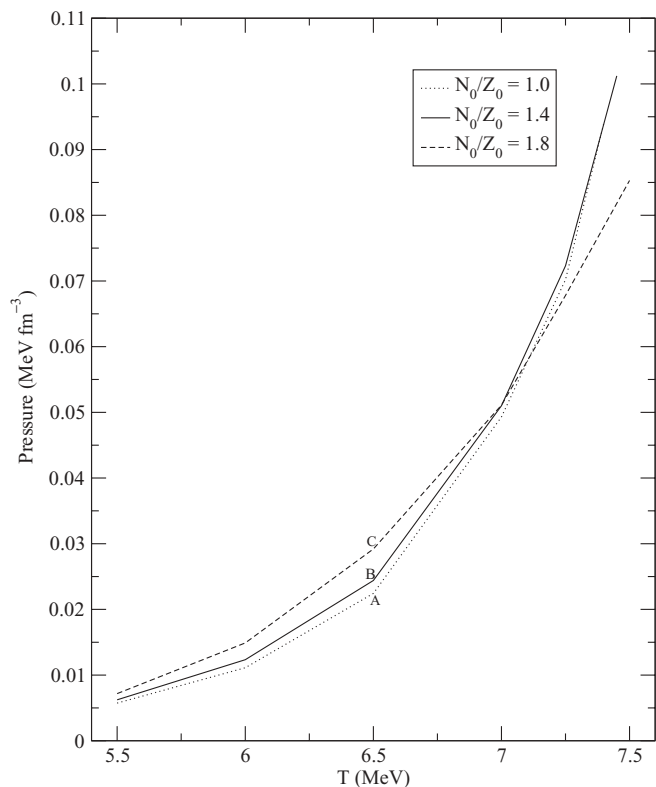


FIG. 7. Phase-coexistence lines in the p - T plane for different values of N_0/Z_0 . As in Fig. 6, points A, B, and C give the value of pressure where coexistence sets in at $T = 6.5$ MeV.

(Fig. 7). Notice that while the coexistence lines for differing asymmetries are different, they are quite similar. As usual, points to the left and above the coexistence lines are in the liquid phase, and points to the right and below are in the gas phase.

The highest point of a coexistence line in the T - p plane usually identifies critical values T_c , p_c [10]. This is not true in Fig. 7. As we consider higher temperatures, points A, B, and C (Fig. 6) will move to the right and up. They will reach the $\rho/\rho_0 = 0.5$ line. These define the end points T , p in Fig. 7. We do not continue to higher densities, because the simple approximation of excluded volume as a means of incorporating interactions between clusters becomes progressively worse. If we accept the validity of the simple multifragmentation model in the region $\rho/\rho_0 \leq 0.5$, we will have to conclude that the critical point does not exist in the region $\rho/\rho_0 \leq 0.5$. The same conclusion can be reached from other published work. Multifragmentation with one kind of particle was also studied by Bugaev *et al.* [11]. This is the same physics problem as considered in Ref. [2] but treated in a different mathematical framework, and these authors considered all densities, not just $\rho/\rho_0 \leq 0.5$. They found that one can identify a critical point at $T = T_c = 18.0$ MeV, $\rho/\rho_0 = 1$, and $p_c = \infty$. At very high pressure, the model must break down, but this is an additional confirmation that the simple multifragmentation model in the domain $\rho/\rho_0 \leq 0.5$ does not contain the critical point.

VII. ISOTHERMALS IN A TWO-COMPONENT SYSTEM

Figure 6 gives the isothermals for $N_0/Z_0 = 1, 1.4,$ and 1.8 at 6.5 MeV temperature. Drawing isothermals for fixed N_0/Z_0 is physically relevant. We are assuming that we have a very large system with given numbers N_0, Z_0 whose volume can change depending upon the physical conditions it is subjected to. If we want to study a different asymmetry, we change N_0/Z_0 accordingly and repeat the calculation. To have a complete knowledge, calculations should be done for all relevant N_0/Z_0 . The most asymmetric system we study is $N_0/Z_0 = 1.8$. Of course, since we have no Coulomb force, the system with $N_0/Z_0 = \alpha$ has the same thermodynamic properties as the system with $Z_0/N_0 = \alpha$.

It is, however, instructive to consider isothermals of two-component systems in a more general fashion. In a one-dimensional system, there is only one density and an isotherm is a line in the p - ρ plane. Now we have two densities ρ_n and ρ_p , and isothermals become surfaces. Let ρ_p be the x axis, ρ_n the y axis, and p the z axis, the equation of state at a given temperature is a surface in this space. A projection of this surface in two dimensions can be made, but for a quantitative study it is more convenient to present contours of constant p in the ρ_p - ρ_n plane. Such a plot is shown in Fig. 8. We consider pressure contours in the region bounded by $\rho_p = 1.8\rho_n$, $\rho_n = 1.8\rho_p$, and $(\rho_n + \rho_p)/\rho_0 \leq 0.5$. The reasons for choosing these boundaries were explained before.

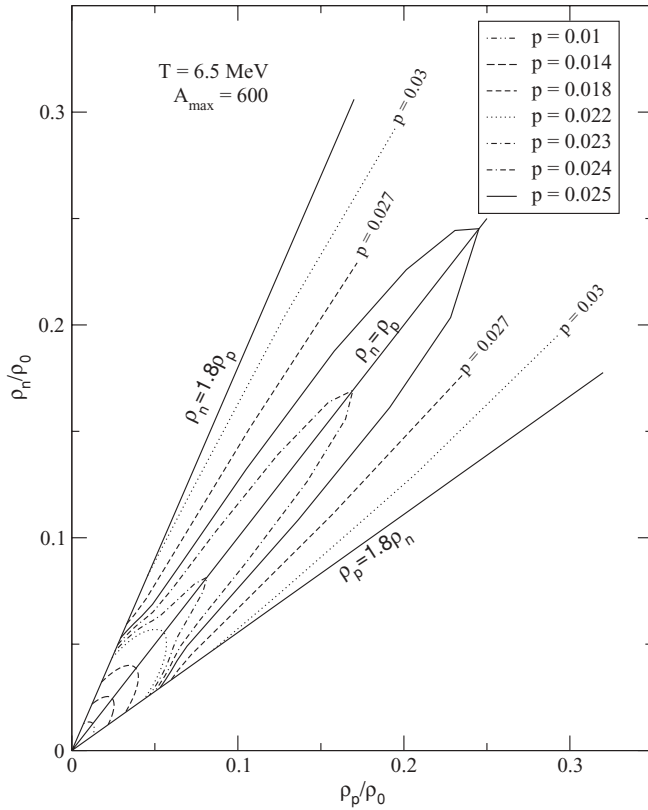


FIG. 8. Contours of constant pressure p in the ρ_n - ρ_p plane at $T = 6.5$ MeV for $A_{\max} = 600$. The values of the pressure (in MeV/fm³) are marked against the contours, and some are given in the box in the upper right corner. The region is bounded by $\rho_n = 1.8\rho_p$, $\rho_p = 1.8\rho_n$, and $(\rho_n + \rho_p)/\rho_0 \leq 0.5$. The line $\rho_n = \rho_p$ is shown in the middle.

Roughly speaking, the contours are either largely radial or circular. Let us first consider an uninteresting gas. We assume it consists of only neutrons and protons and unlike in the present problem does not form composites. In such a case, constant pressure curves would be $\rho_n + \rho_p = \text{constant}$, and these would be straight lines making an angle of $\pi/4$ with the x and y axes. Instead, we see at low ρ_n and ρ_p (when one has a gas phase only) not straight lines but more like concentric circles. This is because pressure is directly proportional to multiplicity (Sec. III) and multiplicity is a function of asymmetry. In our case, composites are present in the gas phase, and the number of composites depends upon the asymmetry of the system. This causes constant pressure contours in the gas phase to bend from straight lines. We skip the details as to why the lines become like circles. We now try to explain other pressure contours that are largely radial. For this, refer back to Fig. 6. We mentioned before that in the limit $A_{\max} \rightarrow \infty$, the p - ρ curves would have zero slopes to the right of points A, B, and C on the isothermals. In such a case, the constant pressure contour would move exactly radially inward from the boundary $\rho/\rho_0 = 0.5$ and would later leave the radial pattern, bend, and finish at the boundary $\rho_n = 1.8\rho_p$ or $\rho_p = 1.8\rho_n$, whichever is appropriate. Similar behavior is seen in Fig. 8. Thus radial pressure contours reflect regions of coexistence.

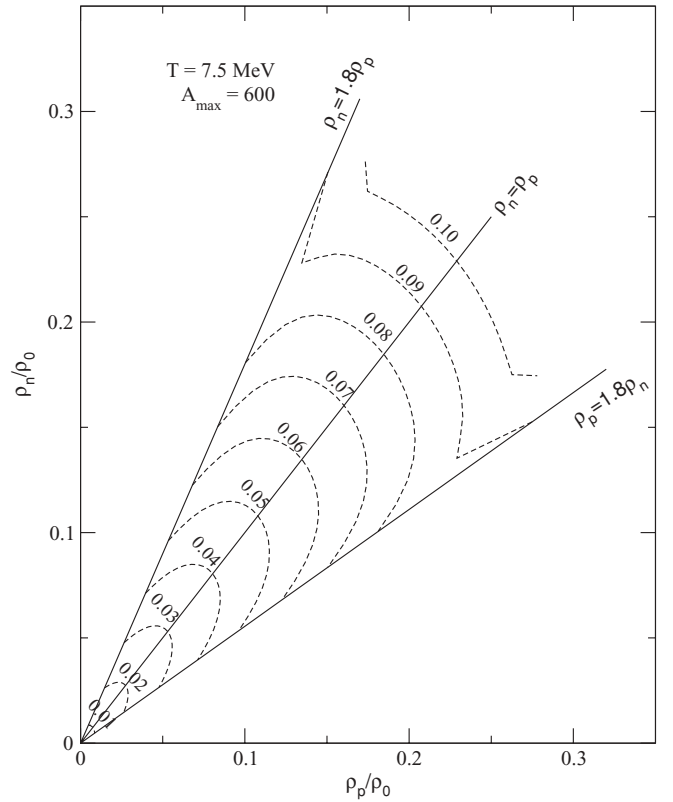


FIG. 9. Same as in Fig. 8, except that the temperature is 7.5 MeV. The system is mostly in the gaseous phase, which changes the shape of the contours here as compared to those in Fig. 8.

As another example, we show in Fig. 9 the pressure contours at $T = 7.5$ MeV. Except near the edges of the boundaries, a pure gas phase is seen.

VIII. ISOSPIN FRACTIONATION

We illustrate isospin fractionation in the multifragmentation model through an example. Consider multifragmentation of a neutron-rich system: $N_0/Z_0 = 1.4$ and temperature $T = 6.5$ MeV. At low density, the system is in a pure gas phase. Following the discussion in Sec. IV, the gas phase consists of light particles with $A \leq 70$ and the liquid phase consists of particles with A between $A_{\max} - 70$ and A_{\max} . At higher density, both gas and liquid phases are seen (Figs. 2 and 3). In the present example with $N_0/Z_0 = 1.4$, we expect that during coexistence the neutron to proton ratio in the gas phase will rise above 1.4 and the neutron to proton ratio in the liquid phase will fall below 1.4. The reason for this is the symmetry energy which preferentially favors formation of larger clusters closest to maximum stability (i.e., $N = Z$). This rise of the neutron to proton ratio in the gas phase is illustrated in Fig. 10. Coexistence sets in a little beyond $\rho/\rho_0 = 0.1$. Until that point is reached, the neutron to proton ratio in the gas phase is at 1.4, the ratio of the parent system. Then as the density increases the ratio increases.

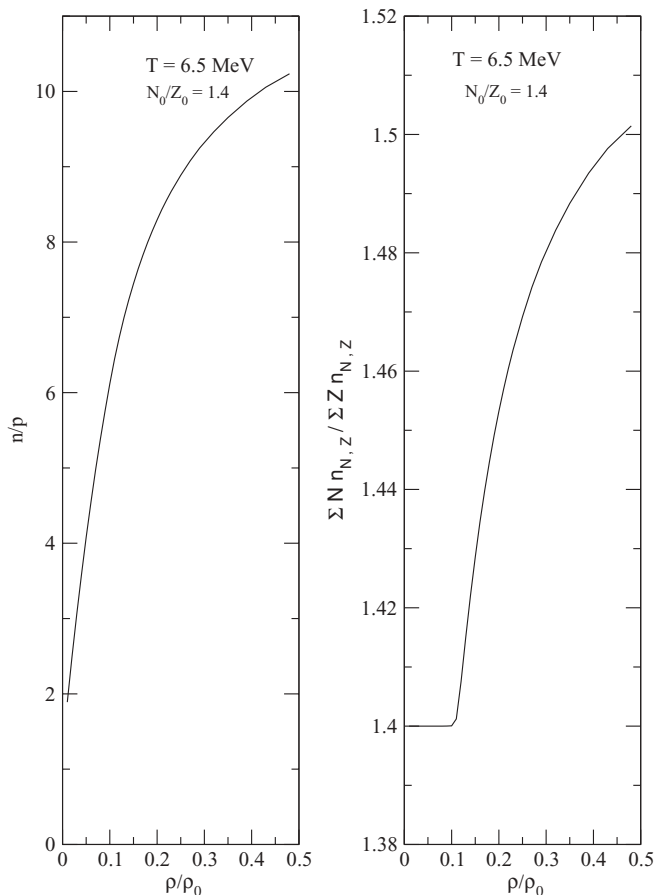


FIG. 10. For $T = 6.5$ MeV and $N_0/Z_0 = 1.4$. The left panel shows the rise of the ratio of the number of free neutrons to the number of free protons as a function of density. While the rise is fast, nothing particularly new happens at the onset of coexistence. If, however, the gas phase is defined to be all particles with $A \leq 70$ (this would be consistent with Figs. 2 and 3), the ratio of neutrons to protons bound in the gas phase remains that of the parent system until coexistence sets in (right panel) and then begins to rise. It behaves like an order parameter if the parent system is asymmetric.

Figure 10 also shows that even at very low density, the ratio of unbound single neutrons to unbound single protons rises very rapidly. But this has nothing to do with what is called isospin fractionation. In fact, nothing special happens to this ratio when coexistence sets in. It is only when the gas phase is considered to include not just single nucleons but also light particles that isospin fractionation becomes an order parameter if $N_0/Z_0 \neq 1$.

In the present example, at $\rho/\rho_0 = 0.35$, the neutron to proton ratio in the gas phase is 1.485. In the liquid phase, it is 1.375.

Isospin fractionation in mean-field theories is treated in Refs. [4,5]. Calculations in the lattice gas model can be found in Ref. [12]. A very pertinent experimental paper [13] discusses the enhancement of the neutron number to proton number but without any isospin fractionation.

IX. DISCUSSION

The multifragmentation model, so useful for fitting experimental data in intermediate energy collisions, leads naturally to a model of phase transition for nuclear matter. In a range of temperature and density, first-order phase transition occurs. The gas and the liquid phases can be clearly identified. This is really remarkable. The model of nuclear multifragmentation may be unique in this respect. The gas phase consists of light nuclei with A up to about 70. Besides these gas particles, there are large blobs of matter (liquid) with mass numbers close to A_{\max} with $A_{\max} \rightarrow \infty$. The model is appropriate at subnormal nuclear density. Modifications of the simple model are needed to extend the model to higher density, but this may not be easy.

Horowitz and Schwenk [14] have made an elegant study of nuclear matter at very low densities (0.02 fm^{-3} or less). In our pertinent range (up to 0.08 fm^{-3}), this is a small density range at the lowest end. The basic models are similar, so the pressures are similar in the overlapping range, but there are differences. In Ref. [14], only neutrons, protons, and α particles are included, and interactions between them are taken into account using the virial expansion. In our case, interactions between composites are not included but all composites are allowed; but in a very dilute case and at not too low temperatures, heavier composites may have a very low probability of occurrence, and so the results would naturally be similar to those in Ref. [14].

Actual nuclear systems as created in heavy ion collisions are finite and in addition have Coulomb forces. This makes identification difficult of signals that are finger prints of the phase transition. This continues to be the subject of intense study, and there is a large volume of literature on this topic. Even though this is outside the scope of the present article, we make a few pertinent comments.

For arbitrarily large systems, such as studied in this paper, at coexistence there are light gas particles whose yields fall with mass number A and ultimately disappear. Then there is essentially a “desert” (no yield) as a function of A , at the end of which there is a very large blob. In finite systems, there is no desert. For these, at coexistence, the yields of very light particles will fall with A . But instead of falling to zero, they rise again as the value of A approaches the mass A_0 of the disintegrating system. This is the well-known U shape. Examples of this can be found at many places, for example, Fig. 1 in Ref. [7]. The details of the U shape depends upon the energy of collision. As the collision energy increases, the temperature will rise, and the yield of the maximum at the high A side will begin to decrease and finally will disappear. The temperature at which this happens can be thought of as the “boiling temperature” of this finite system.

There are other signals that have been thought of and used. But these are not very directly related to the work reported here so we omit those aspects.

ACKNOWLEDGMENTS

Work reported in Sec. VII had its origin from discussions with F. Gulminelli during a past collaboration.

We acknowledge a communication with S. Samaddar. We acknowledge generous computation help from J. Gallego.

This work is partially supported by the Natural Sciences and Engineering Research Council of Canada.

-
- [1] P. Bhattacharyya, S. Das Gupta, and A. Z. Mekjian, Phys. Rev. C **60**, 064625 (1999).
- [2] G. Chaudhuri, S. Das Gupta, and M. Sutton, Phys. Rev. B **74**, 174106 (2006).
- [3] J. N. De and S. K. Samaddar, Phys. Rev. C **76**, 044607 (2007).
- [4] H. Muller and B. D. Serot, Phys. Rev. C **52**, 2072 (1995).
- [5] C. Ducoin, Ph. Chomaz, and F. Gulminelli, Nucl. Phys. **A771**, 68 (2006).
- [6] S. Das Gupta and A. Z. Mekjian, Phys. Rep. **72**, 131 (1981).
- [7] C. B. Das, S. Das Gupta, W. G. Lynch, A. Z. Mekjian, and M. B. Tsang, Phys. Rep. **406**, 1 (2005).
- [8] J. P. Bondorf, A. S. Botvina, A. S. Iljinov, I. N. Mishustin, and K. Sneppen, Phys. Rep. **257**, 133 (1995).
- [9] A. Botvina, G. Chaudhuri, S. Das Gupta, and I. Mishustin, Phys. Lett. **B668**, 414 (2008).
- [10] F. Reif, *Fundamentals of Statistical and Thermal Physics* (McGraw-Hill, New York, 1965), Chap. 8.
- [11] K. A. Bugaev, M. I. Gorenstein, I. N. Mishustin, and W. Greiner, Phys. Rev. C **62**, 044320 (2000).
- [12] Ph. Chomaz and F. Gulminelli, Phys. Lett. **B447**, 221 (1999).
- [13] L. G. Sobotka *et al.*, Phys. Rev. C **62**, 031603(R) (2000).
- [14] C. H. Horowitz and A. Schwenk, Nucl. Phys. **A776**, 55 (2006).